Optimal PV and Battery Sizing for a Space Microgrid Near the Lunar South Pole Considering ISRU, Habitat and Water Subsystem Power Demand

Saha, Diptish; Bazmohammadi, Najmeh; Vasquez, Juan C.; Guerrero, Josep M.

Published in:
52nd International Conference on Environmental Systems

Publication date:
2023

Document Version
Publisher's PDF, also known as Version of record

 ICES-2023-250

Optimal PV and Battery Sizing for a Space Microgrid Near the Lunar South Pole Considering ISRU, Habitat and Water Subsystem Power Demand

Diptish Saha [1], Najmeh Bazmohammadi [2], Juan C. Vasquez [3] and Josep M. Guerrero [4]
Aalborg University, Aalborg, Denmark

The size and mass of the payload substantially affect the cost of space missions. The aim of this paper is to investigate the optimal mass and size of the photovoltaic (PV) array and battery in a PV-battery-powered lunar microgrid (MG) at 15 highly illuminated candidate sites near the lunar south pole. It is assumed that PV arrays are installed on top of towers with a height of 10 m. The methodology to estimate the PV output power at each candidate site using the illumination time-series profile is presented. On the consumption side, the power demand profiles of ISRU and wastewater subsystems are determined using the estimated oxygen and water consumption profiles of the habitat with four crew members. The closed-loop model of water management includes the interaction of ISRU, wastewater filtration system, and the crew habitat. The power consumption profile of the crew habitat is generated considering different power-consuming components in the habitat as well as the daily schedule of the crew members. Organizing different loads in a multi-microgrid system is also investigated. Finally, a criterion, mass-per-unit-load (MPUL), is used to compare different sites and select the best location with the minimum PV-battery system mass that can serve the highest power demand.

Nomenclature

AWP alternative water processor.

DW drinking.

EPS electrical power system.

ESS energy storage system.

FR food rehydration.

ISRU in-situ resource utilisation.

ISS International Space Station.

LSS life support system.

MG microgrid.

MMG multi-microgrid.

PH personal hygiene.

PV photovoltaic.

RFC regenerative fuel cell.

SH shower.

SoC state-of-charge.

UF urinal flush.

UPA urine processor assembly.

WPA water processor assembly.

α	Sun elevation angle $[rad]$
β	Array inclination angle $[rad]$
χ_d	Dust on the PV panels [%]
η_{sc}	PV cell efficiency [%]
A_a	PV array area $[m^2]$
f_{sc}	PV cell fill factor [%]
I_s	Solar intensity $[W/m^2]$
P^t_{ISRU}	Hourly ISRU total power demand $[W]$
P^t_{PV}	Hourly PV power $[W]$
$P^t_{V_{ir}}$	Hourly ISRU power demand $[W]$
V_{ir}	Hourly fraction of the reactor volume replenished with ilmenite $[1/h]$

[1] Ph.D. Student, AAU Energy, Aalborg University, Denmark; email: dsa@energy.aau.dk
[2] Assistant Professor, AAU Energy, Aalborg University, Denmark; email: naj@energy.aau.dk
[3] Professor, AAU Energy, Aalborg University, Denmark; email: juq@energy.aau.dk
[4] Professor, AAU Energy, Aalborg University, Denmark; email: joz@energy.aau.dk

I. Introduction

A human base on the Moon requires a reliable and efficient electrical power system (EPS) to supply the power demand of different power-consuming units. The power-consuming units in the base primarily consist of crew habitat, to live and perform scientific experiments, and in-situ resource utilisation (ISRU), to produce oxygen and water using the local resources such as lunar regolith. The EPS of the lunar base consist of several interconnected power-demanding systems, power generating sources, and energy storage system (ESS), which can be called space microgrids (MGs) on the Moon or lunar MGs[1,2]. The harsh space conditions entail developing a reliable and resilient MG ensuring power supply even during critical emergencies to support human life and maintain communication with the ground station. Taking inspiration from the terrestrial systems, several power-consuming units in a lunar base may be distributed between several MGs to have their own power generation and ESS and form an multi-microgrid (MMG) system. The MMG systems come with the benefits of sharing resources among several MGs, and increasing the reliability and resiliency of the power system. Taking into account similarities of terrestrial and lunar MGs, several solutions developed for terrestrial MGs can be adapted to be applied to lunar MGs and vice versa[2,3].

On the Moon, electricity can be generated from several resources, such as solar radiation, nuclear reactors[4], and electrostatic charge from the regolith[5]. Although nuclear reactors provide light, small, modular, and site-independent solutions, their installation requires serious considerations to limit the nuclear radiation exposure of the crew members, for instance, through maintaining an appropriate distance between the reactors and the habitat, or employing suitable shielding[4]. In the former case, appropriate ways for transferring the power from the generation site to the base[6] are needed, while in the latter, displacement of lunar regolith might be required[4]. Transportation of additional equipment in the form of power cables or heavy machinery increases the payload, and thereby the mission cost. Safe disposal of nuclear waste is also a serious issue. On the other hand, generating power from the electrostatic charge of the lunar regolith is still undergoing laboratory tests[5]. The absence of an atmosphere on the Moon permits ample solar energy to reach the lunar surface, and solar radiations are not affected by atmospheric disruptions such as cloud coverage and diffusion. Solar power generation technology is well tested on Earth and in several space missions. It does not require safe distance consideration and allows easy expansion, thereby providing an efficient solution for generating electrical power on the Moon.

Generating power from photovoltaic (PV)-arrays requires adequate solar illumination at the lunar base site. Several highly illuminated sites near the lunar polar regions have been identified in previous studies using the average illumination information[7–9]. Several studies investigate installing PV arrays on top of high towers to increase the average available illumination[10]. Designing such solar array structures is currently under consideration by several space agencies[11,12]. It is observed that installing PV arrays on top of towers reduce the ESS requirements[10]. In general, space mission costs are directly proportional to mass. Therefore, reducing the size of the ESS reduces the space mission cost. There are several ESS technologies for space applications[1]. In Ref. 13, batteries and regenerative fuel cell (RFC)-based ESS assisted with PV arrays are compared for a period of 10 years from 2020 to 2030[13]. It is observed that despite PV-RFC system having lower overall mass, batteries have higher efficiency than RFCs[13]. According to Ref. 4, the mass of the battery for a PV-battery system supplying an ISRU system located at 30° latitude with a total power demand of $25.8\ kW$ is approximately $58,000\ kg$. Non-polar regions receive roughly 15 days of uninterrupted sunlight followed by approximately 15 days of uninterrupted nighttime[14]. Therefore, the size of the ESSs increases as ESSs must supply the power required by the critical loads during the night time. Although polar regions possess high average illumination, there are high terrains around polar regions according to the data collected by *NASA's Lunar Reconnaissance Orbiter (LRO)*[15,16]. Moreover, the solar elevation angle close to polar regions is less than 10°. The low solar elevation angle and high terrains create long shadows[10,17] obstructing the solar radiation to reach the Moon's surface. Therefore, the solar illumination time-series profile at each location should be determined considering the nearby topography along with the Sun elevation angle to have an approximation of the available power from the Sun for planning and operation management of MGs[18].

This paper presents a comparison study for a PV-battery based MG considering the size of the PV array and battery size and mass at 15 candidate sites (see Table 1[7–9,18]) near the lunar south pole for a period of one lunar month ($\sim 708\ h$). It is common practice to model the power budget of space missions as a fixed value equal to the average or peak power demand of power-consuming units. However, the power demand depends on the operating mode and the rate of operation of the unit. For instance, the oxygen and water requirement of the base depends on several daily activities of the crew members. In addition, the power consumption of the wastewater filtration subsystem depends on the rate of wastewater generation in the base. The power consumption profiles of different power-consuming units are required for the operation management of the base. In this paper, the power demand profile of the ISRU is determined

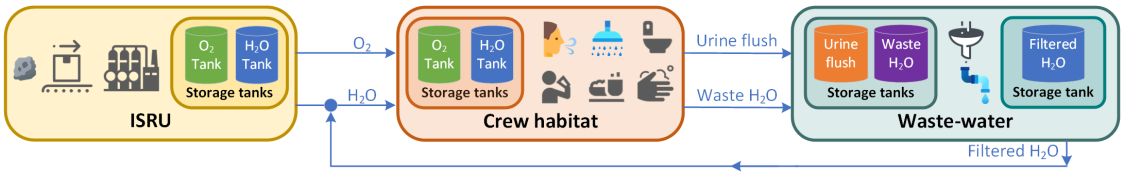

Figure 1. The interacting subsystems in a lunar base for maintaining the oxygen and water flow.

according to the oxygen and water management of the base considering three interacting subsystems, namely ISRU, crew habitat, and wastewater filtration system. To the best of our knowledge, such a comparison study to investigate the mass of a PV-battery MG at different highly illuminated candidate sites near the lunar south pole has been not reported in the literature. In this paper, the power demand profile of the habitat is generated considering the daily activities of the crew members. It is assumed that ISRU and habitat have their own MG system to enhance the reliability of the base. The sites are also compared with respect to the longest continuous nighttime, average illumination, total power demand served, total PV power generated, and mass-per-unit-load (MPUL) criterion to identify the sites serving the highest power demand with the least total PV-battery systems mass.

The rest of this paper is organized as follows. The optimal power demand profiles of both ISRU and habitat MGs are investigated in Section II considering the long-term operation objective of the lunar base and several daily activities of the crew members. The optimal PV array and battery size required to supply the power demand of the PV-battery MG for ISRU and habitat are discussed in Section III. The comparison study in terms of the mass and size of PV array and battery for the 15 highly illuminated sites near the lunar south pole, Shackleton crater, is presented in Section IV. Finally, concluding remarks are given in Section V.

Table 1. Location of 15 highly-illuminated candidate sites.[7–9,18]

Site #	Longitude	Latitude
1	222.6627	−89.4511
2	222.6415	−89.4333
3	222.8084	−89.4390
4	203.6490	−89.7797
5	203.2861	−89.7731
6	37.1013	−85.2963
7	123.7604	−88.8084
8	197.1382	−89.6866
9	222.4191	−89.4407
10	37.0207	−85.2897
11	291.7803	−88.6704
12	197.7447	−89.6884
13	202.8645	−89.7624
14	222.5634	−89.4734
15	222.7638	−89.4502

II. ISRU and habitat power demand profile

A. ISRU power demand profile

For sizing the PV array and battery for the PV-battery MG, an estimation of the required power demand to be served is essential. In this paper, it is assumed that there are two MGs, one for the ISRUs and another for the habitat, each having its own PV array and battery. The power demand profiles obtained for ISRU and habitat are discussed in the following subsections.

In this paper, the closed-loop model of oxygen and water, including the interaction between the ISRU, crew habitat, and wastewater filtration system, is considered, as shown in Figure 1. The water and oxygen for the lunar base are produced by the ISRU utilizing the lunar regolith. The power consumption of the ISRU depends on the rate of intake of regolith (V_{ir}) as shown in Figure 2[4]. The ISRU produces water by performing catalyzed hydrogen reduction reaction of the regolith in a reactor, which is then electrolyzed to produce oxygen[4]. Therefore, both oxygen and water are generated with the intake of regolith. Electrical power is consumed by the electrical motors for scooping, transporting, vibrating, separating, and transferring regolith and performing electrolysis. The reactor requires thermal energy to perform the reduction reaction, which is assumed to be supplied by electrical heaters in this paper. Therefore, the total power consumption of ISRU shown in Figure 2 also includes the electrical power that is required by electrical heaters. In addition, reusing and recycling available resources are encouraged in an environment with a scarcity of resources. Thus, instead of depending on ISRU for all the water demands of the habitat, a wastewater subsystem is considered in the habitat that can filter the habitat wastewater and produce clean water for further use.

For the operation management of the habitat, it is necessary to calculate the daily oxygen and water consumption and wastewater generation profiles of the habitat. The amount of oxygen and water consumption and wastewater generation for different activities for one crew member is listed in Table 2. It is considered that four crew members are

present in the habitat carrying out their daily activities. The daily oxygen and water consumption profiles, as shown in Figure 3a and Figure 3b, respectively, are created according to the daily schedule of the crew members as described in Table 3 and their consumption rates as listed in Table 2. The daily urine and wastewater generation profiles for four crew members are shown in Figure 3c and Figure 3d, respectively. The daily oxygen and water consumption and wastewater generation profiles are repeated for the whole mission duration of 1 month ($\sim 708\ h$).

The oxygen and water requirements in the habitat are fulfilled by respective tanks in the habitat. The desired level of the habitat's oxygen tank is maintained by refilling oxygen from the ISRU oxygen tank, while the desired level of the habitat's water tank is maintained by refilling water from both the ISRU and wastewater filtration system water tanks as shown in Figure 1. Whenever the actual level of oxygen and water in the ISRU tanks deviates from the desired level, V_{ir} is adjusted accordingly to reach the desired level. A multi-objective optimization function is formulated to follow the desired levels of the oxygen and water tanks of ISRU and habitat, as shown in Figure 4b, Figure 4d, Figure 4e, Figure 4f, and Figure 4g. The solution to the optimization problem determines the maximum rate at which the oxygen is transferred from the ISRU to the habitat oxygen tank, the maximum rate at which the filtered freshwater is transferred from the wastewater system to the habitat water tank, the hourly maximum rate at which water is transferred from ISRU to the habitat water tank, and the hourly V_{ir} to produce oxygen and water for the complete optimization horizon. The amount of V_{ir} determines the hourly power demand of the ISRU (see Figure 4c) according to the methodology proposed in Ref. 4(sec. 3.1, p. 10). Therefore, the power demand of ISRU depends on the crew members' oxygen and water consumption rates. The PV power profile is obtained from the Sun illumination time-series profile considering the Sun, Earth, and Moon three-body system proposed by the authors in Ref. 18. The Sun illumination time-series profile is used to generate the PV power profile (P^t_{PV}) as follows[2,4]:

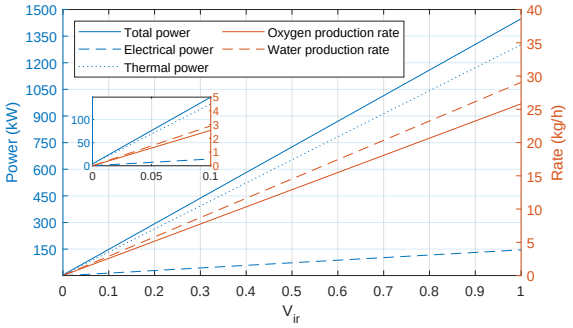

Figure 2. ISRU power demand variation and oxygen and water production rates with varying V_{ir}. Inset figure shows the variation with V_{ir} from 0 to 0.1.

$$P^t_{PV} = (1 - \chi_d) f_{sc} \eta_{sc} A_a I_s \sin(\alpha + \beta) \tag{1}$$

where χ_d is assumed to be 0 % considering that the PV arrays are installed near the base and are cleaned periodically, f_{sc} is assumed to be 89 %, and η_{sc} is assumed to be 28 %. I_s is assumed to be $1359\ W/m^2$, which is multiplied by the Sun illumination time-series profile[18] following the methodology proposed in Ref. 2. The amount of α is calculated using the methodology proposed in Ref. 2 and Ref. 4(sec. 5.1, p. 35), while β is assumed to be equal to the latitude of the site, which is $89.78°$. The PV output power with an optimal A_a of $294.95\ m^2$ is shown in Figure 4a. The PV power at a site is also not continuously available as shown in Figure 4a. Therefore, it is assumed that the ISRU stops its operation when PV power is unavailable at the site, as shown in Figure 4c, since ISRU is a high-power demanding system that increases the battery's size for operation during the dark period. If there is a long dark period in the near future, the ISRU operation management system decides to produce more oxygen and water to be prepared for the upcoming no-operation period utilizing the available energy during the illuminated period. The optimization problem results in an optimal power consumption profile for maintaining the desired levels in the oxygen and water tanks of ISRU considering the long-term safe operation of several interacting subsystems of the base.

It is assumed that, apart from the power consumption for processing the regolith to produce oxygen and water, ISRU also consumes power for running several other types of equipment as listed in Table 4[2,4,14,20]. It is assumed that power-consuming units are in the active operating state when solar energy is available. During dark periods, it is assumed that they are in survival operating mode consuming low/idle power. From Table 4, it is calculated that the total active and survival power consumption of different types of equipment in ISRU is approximately 11 kW and 8 kW, respectively. Therefore, the total power consumption profile of ISRU is calculated as:

$$P^t_{ISRU} = \begin{cases} P^t_{V_{ir}} + 11000 & P^t_{PV} > 0 \\ P^t_{V_{ir}} + 8000 & P^t_{PV} = 0 \end{cases} \tag{2}$$

The total power demand profile of ISRU including the power required by supporting devices is shown in Figure 4h.

Table 2. The water and oxygen consumption and wastewater generation rates for different activities for one crew member. [19] **[Table 4-20 (p. 72), Table 3-25 (p. 49), Table 4-21 (p. 73)]**

Water consumption (kg/day)		Oxygen consumption (g/min)		Wastewater generation (kg/day)	
Activity	Amount	Activity	Amount	Activity	Amount
Drinking (DW)	2.00	Sleep	0.37	Urine	1.50
Food rehydration (FR)	0.50	Nominal	0.59	Oral hygiene	0.37
Urinal flush (UF)	0.50	Exercise	3.99	Hand wash	4.08
Personal hygiene (PH)	0.40	Exercise recovery	0.59	Shower	1.08
Shower (SH)	1.08	Pre/Post-sleep	0.59	Crew latent humidity condensate	2.27

Table 3. Daily schedule of the crew members used for generating the oxygen and water consumption profiles.

Time (h)	Water consuming activity	Oxygen consuming activity
00:01 - 06:00	None	Sleep
06:01 - 07:00	DW + PH + UF + FR + SH or DW + PH + UF + FR	Post-sleep (Nominal)
07:01 - 08:00	None	Exercise
08:01 - 09:00	DW	Exercise recovery
09:01 - 12:00	None	Nominal
12:01 - 13:00	DW + PH + UF + FR	Nominal
13:01 - 15:00	None	Nominal
15:01 - 16:00	DW + UF	Nominal
16:01 - 18:00	None	Nominal
18:01 - 19:00	DW + PH + UF + FR or DW + PH + UF + FR + SH	Nominal
19:01 - 21:00	None	Nominal
21:01 - 22:00	DW + PH + UF	Pre-sleep (Nominal)
22:01 - 00:00	None	Sleep

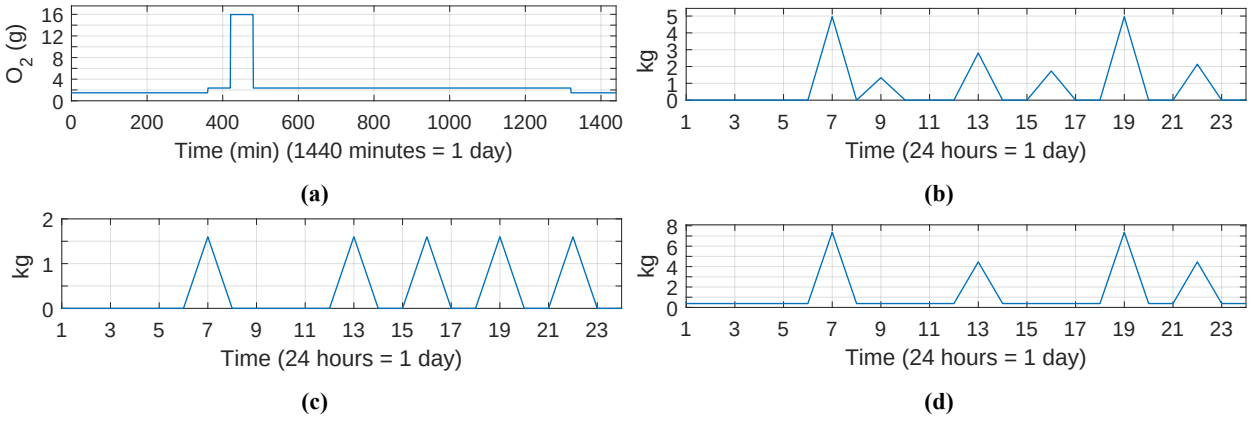

Figure 3. Daily (a) oxygen consumption (b) water consumption, (c) urine wastewater generation, and (d) wastewater generation profiles for four crew members

B. Habitat power demand profile

Several devices consume power in the habitat for maintaining the artificial atmosphere, life support system (LSS), wastewater treatment, exercising, performing scientific experiments, charging electric vehicles and rovers, and communicating within the base and the ground station on Earth, among others. The wastewater subsystem in the habitat is responsible for extracting filtered water for reuse from the wastewater produced in the habitat. Considering the requirements of a lunar base, a wastewater filtration process named alternative water processor (AWP) is presently in the development stages[21–23]. Currently, the water recovery system in the International Space Station (ISS) consist-

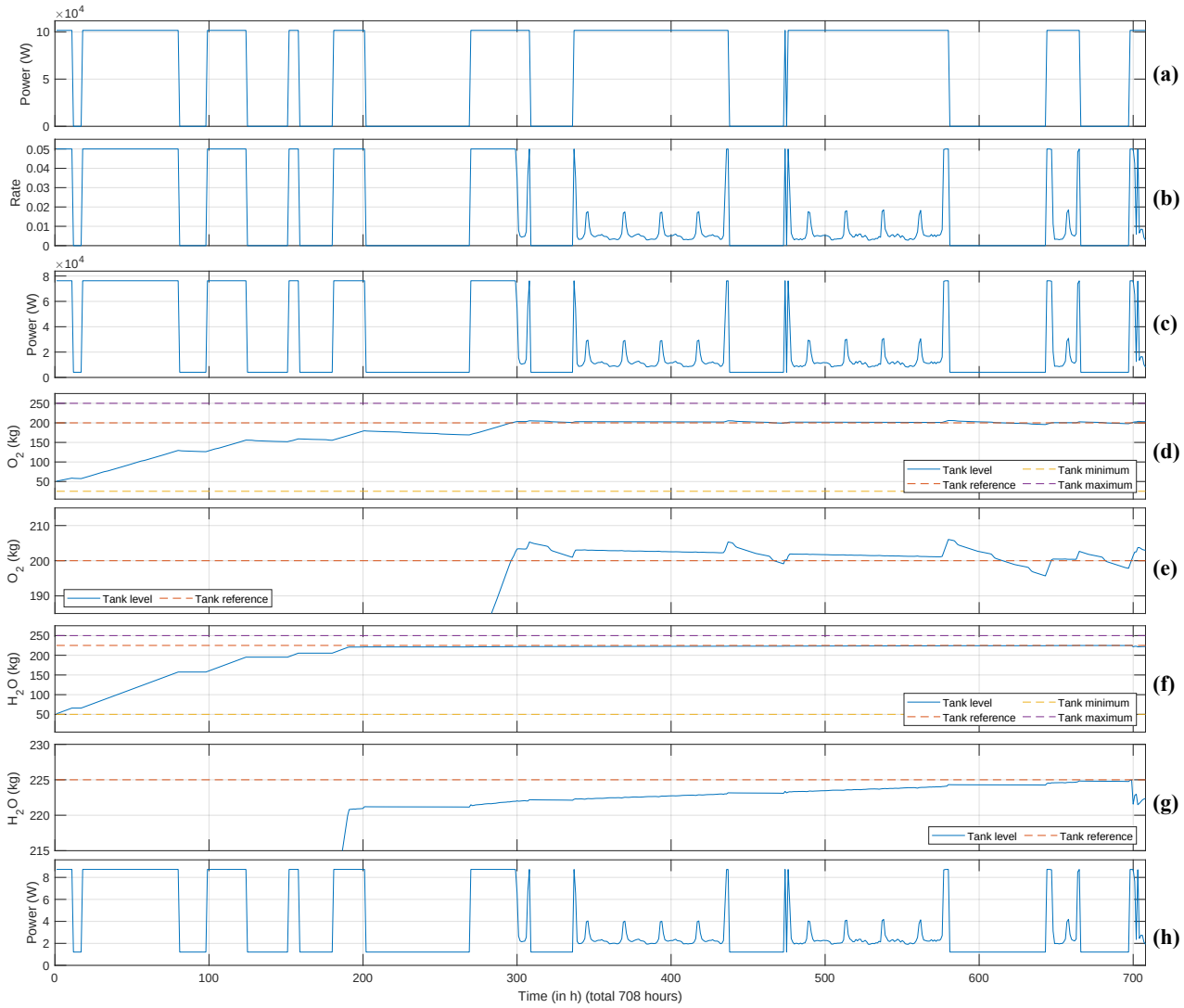

Figure 4. (a) Optimal PV power generation for ISRU MG at site #4 (longitude $203.6490°$ and latitude $-89.7797°$) with an array area of $294.95\ m^2$ near the Shackleton crater from July 6, 2023, to August 5, 2023 (b) Intake rate of lunar regolith (c) ISRU power consumption (d) ISRU oxygen tank level (e) ISRU oxygen tank level zoomed (f) ISRU water tank level (g) ISRU water tank level zoomed (h) ISRU power demand with several supporting devices.

ing of urine processor assembly (UPA) and water processor assembly (WPA) is responsible for filtering the generated urine wastewater and wastewater, respectively[24]. In the operational mode, the UPA and WPA require $315\ Wh/h$ and $320\ Wh/h$ power, respectively, along with $108\ Wh/h$ power required by the control modules (in total $743\ Wh/h$). In the standby mode, the ISS water recovery system requires $297\ Wh/h$ of power[25]. The water recovery system can recover 81% of wastewater[25], and it is assumed that the water recovery system can process $2.5\ kg/h$ at a time. The power consumption of UPA and WPA and the wastewater processing capability of the water recovery system are considered to obtain the power-consumption profile of the wastewater subsystem as shown in Figure 5. It is worth noticing that the power-consumption profile of the wastewater subsystem is generated by solving the optimization problem for ISRU power demand as the filtered water from the water recovery system is reused along with the water produced by the ISRU to fulfill the needs of the water in the habitat. The power demand of the wastewater subsystem is assumed to be supplied from the habitat MG as the wastewater subsystem is considered to be a part of the habitat. Three different tanks are considered to store the urine wastewater, wastewater, and filtered water at a desired level as shown in Figure 5b, Figure 5c, and Figure 5d, respectively. An algorithm is developed in this paper to maintain the desired levels of

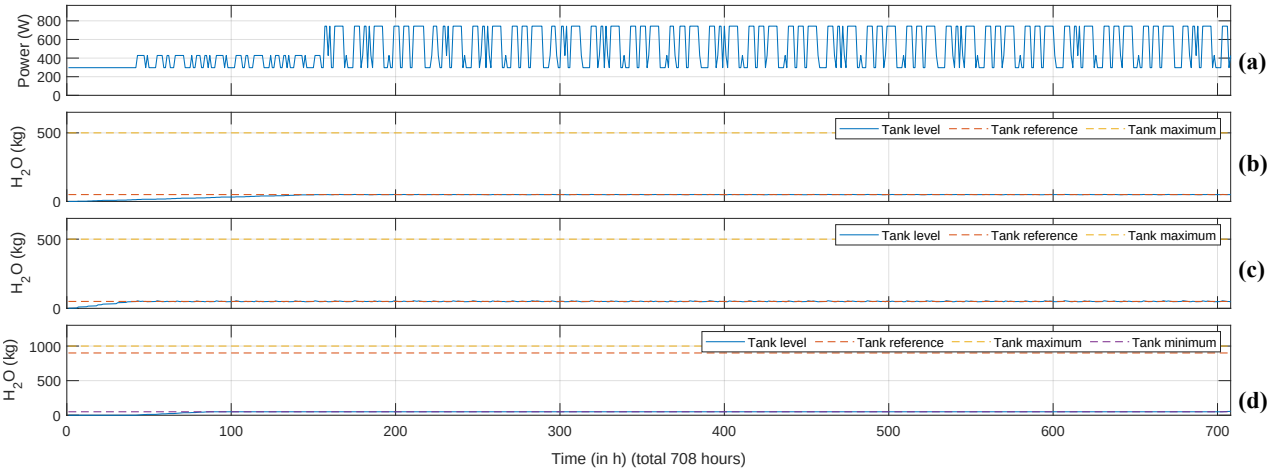

Figure 5. (a) Wastewater subsystem power demand profile (b) Urine wastewater tank content level (c) Wastewater tank content level (d) Filtered water tank content level.

the tanks by taking out water from the urine wastewater and wastewater tanks, using the filtering process, and storing the filtered water. It can be observed from Figure 5c and Figure 5a that as soon as the wastewater tank reaches its desired reference, the wastewater subsystem starts its operation and consumes higher power than the standby power. From Figure 5b and Figure 5a, it can be observed that when the urine wastewater tank reaches its desired reference, both UPA and WPA are operational and consumes a high power of 743 Wh/h. It can also be noticed in Figure 5d that the filtered water tank level is not increasing even though the water recovery system is operational because the filtered water is also transferred to the habitat potable water tank for use by crew members.

The habitat power demand profile is created using the power consumption information of its power consuming units according to their time of use as listed in Table 5[2,4,14,20] and the power consumption profile of the wastewater subsystem as shown in Figure 6. The time of use of these devices is based on the daily activity schedule of the crew members, as mentioned in Table 3. The PV power generation profile in Figure 6 is also generated using Eq. (1) with optimal A_a of 120.28 m^2. Similar to ISRU, the devices in the habitat also consume active-state power while solar energy is available. Several devices are switched off or kept in low/idle (survival)-powered conditions to reduce power consumption from the batteries in the dark period. It can be observed from Figure 6 that the power consumption of the habitat reduces during the period when PV power is unavailable. In Ref. 4, it is estimated that each crew member in the habitat consumes approximately $5-10$ kW of power. In this paper, a total power of approximately 20 kW is considered for a base with four crew members.

Table 4. Different types of power consuming equipment in ISRU.[2,4,14,20]

Equipment	Power (W)	
	Active	Survival
Electrical power system	200	200
Communication system internal components	1500	750
Communication system external components	1000	1000
Central computer	100	100
#9 Monitoring camera	5	5
Air compressor	3.5	3.5
Airlock status LED	5	5
Artificial daylight LED	150	75
Airlock vacuum pump	500	500
#33 Lighting LED lamps	20	10
LCD display	160	0
Lunar day thermal control system	1200	900
Lunar night thermal control system	1900	1500
Sensors	4000	3000
Total	**10743.5**	**8048.5**

The power demand profile for both ISRU and habitat MGs are generated and used to optimally size the PV array and battery for the PV-battery MG of ISRU and habitat as explained in the following section.

Table 5. Power consuming devices in the habitat and their time of use[2,4,14,20]

Device	Active-state power (W)	Survival-state power (W)	Average daily use (h)	Time of use (h)
Air compressor	3.5	3.5	24	0 – 24
Airlock vacuum pump	500	500	1	21 – 22
Airlock status LED	5	5	24	0 – 24
Artificial daylight LED	150	75	24	0 – 24
Water heater - 1	4000	0	1	6 – 7
Water heater - 2	4000	0	1	18 – 19
LSS	4500	3000	24	0 – 24
Induction oven	2000	0	1	8 – 9
Monitoring camera (9 Nos)	5	5	24	0 – 24
Laptop	60	60	12	9 – 21
LCD display	160	0	24	0 – 24
Lighting LED lamps (33 Nos)	20	10	4	20 – 24
Microwave	800	0	2	7 – 9
Projector-1	60	0	1	10 – 11
Projector-2	60	0	1	11 – 12
Crew Laptop-1	65	0	10	8 – 18
Crew Laptop-2	80	0	6	9 – 20
Crew Laptop-3	60	0	3	9 – 21
Crew Laptop-4	80	0	10	8 – 19
Crew Smartphone-1	2	0	1	19 – 20
Crew Smartphone-2	2	0	1	20 – 21
Crew Smartphone-3	5	0	2	19 – 21
Crew Smartphone-4	3	0	2	17 – 19
Camera-1	10	0	2	10 – 12
Camera-2	10	0	1	15 – 16
Camera-3	10	0	1	21 – 22
Camera-4	10	0	1	11 – 12
Camera-5	10	0	1	13 – 15
Camera-6	10	0	1	17 – 18
Treadmill	800	0	1	7 – 8
Refrigerator-1	10	10	24	0 – 24
Refrigerator-2	10	10	24	0 – 24
Hair dryer-1	1200	0	1	6 – 7
Hair dryer-2	1200	0	1	18 – 19
Washing machine	2000	0	1	19 – 20
Vacuum cleaner	1.5	0	1	19 – 20
Electrical power system-1	500	500	24	0 – 24
Electrical power system-2	300	300	24	0 – 24
Communication system internal components	2500	1500	24	0 – 24
Communication system external components	3000	3000	24	0 – 24
Central computer	100	100	24	0 – 24
Spacesuit battery charger	140	140	6	23 – 5
Sample drill battery charger	2000	0	2	21 – 23
Lunar day active thermal control system	1200	900	24	0 – 24
Lunar night active thermal control system	1900	1500	24	0 – 24
Sensors	4000	3000	24	0 – 24
3D printer	700	0	12	9 – 21
Welder	5000	0	1	11 – 12
Laboratory electric arc furnace	5000	0	1	14 – 15
Manufacturing device	2000	0	1	16 – 17
Rover charging	7000	1000	6	23 – 5
Pressurized EV charging	10 000	3000	6	23 – 5
Unpressurized EV charging	3000	2000	6	23 – 5

III. ISRU and habitat PV-battery power profile

The cost of space missions is affected by the mass and stowage area of the payload. Thus, several innovative strategies have been developed to reduce the cost of space missions. In a PV-battery MG, the size and mass of the

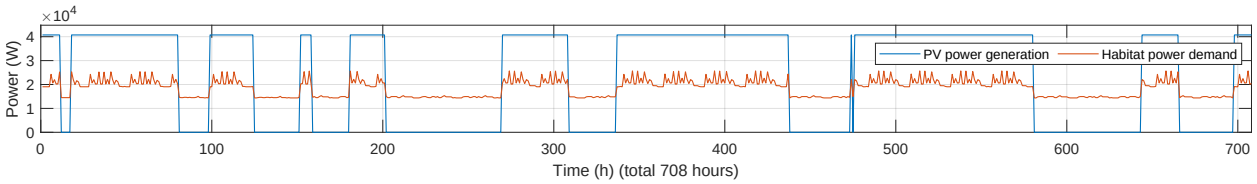

Figure 6. Habitat power demand profile and optimal PV power generation for habitat MG at site #4 (longitude $203.6490°$ and latitude $-89.7797°$) with array area of $120.28\ m^2$ near the Shackleton crater from July 6, 2023, to August 5, 2023.

PV array and battery play a vital role in the cost of the space mission. A multi-objective optimization problem is proposed to minimize the battery and the PV array mass, and maintain the battery state-of-charge (SoC) at a desired level, while minimizing the total unused power from the PV system. Constraints related to the allowable battery charging/discharging power and power balance in the MG are also taken into account[2]. The solution to the optimization problem is the optimal battery capacity, PV array area (A_a), and the hourly excess PV power generation that is shed. It is tried to maintain the battery SoC within 20% and 90% of the maximum battery capacity while following a desired reference level. The excess PV power generation is assumed to be curtailed in this study since storing it in the battery requires an unnecessary increase in the battery size, and, thereby, the battery mass. Instead of shedding the excess PV power, several other power-consuming units in the base can be optimally scheduled to use the excess power, which is the subject of the future study of the authors.

The optimal PV power generation profile from the optimized PV array area of $294.95\ m^2$ and the power demand profile of ISRU MG at site #4 is shown in Figure 7a. During the period when the power generation is more than the demand, the extra generation is either used to charge the battery or shed. The battery is charged if the battery SoC is less than the desired level or the optimization algorithm decides to charge the battery to be prepared for supplying the power demand during the period when PV generation is unavailable, as shown in Figure 7c. The excess PV power generated is shed during the period when the battery SoC reaches its desired level as shown in Figure 7b. The battery charging and discharging power for the ISRU MG is shown in Figure 7d. A similar strategy is adopted for the operation of habitat's PV-battery MG. The optimal PV power generation profile from the optimized PV array area of $120.28\ m^2$ and the power demand profile of habitat MG at site #4 is shown in Figure 7e. The supplied and shed PV power is shown in Figure 7f. The battery SoC and charging/discharging profile for the habitat MG are shown in Figure 7g and Figure 7h, respectively.

IV. Comparative analysis

In this section, the optimal PV array area and battery size and mass for 15 highly illuminated sites listed in Table 1 [7–9,18] near the lunar south pole are found and compared. The optimization horizon is considered $708\ h$ ($= 1$ lunar month). It is assumed that the PV arrays are installed on the top of $10\ m$ high towers. Two PV-battery MGs for ISRUs and crew habitat, are considered each having its own PV and battery systems. Although the two MGs can share their resources, it is not considered in this study.

The optimal battery capacity (Wh) for different candidate sites is shown in Figure 8e. It is observed that the optimal battery size is in the order of $10^6\ Wh$ for both the ISRU and habitat MGs. The mass of the battery can be found from the battery capacity as follows[4]:

$$M_B = \frac{E_{cap}}{S_b B_{dod}} \tag{3}$$

where E_{cap} is the battery capacity (Wh), B_{dod} is the battery depth of discharge set to 80% of the battery capacity, and S_b is the battery specific energy set to $200\ Wh/kg$[4]. It is observed that the battery mass is in the order of $10^4\ kg$ for the individual ISRU and habitat MGs and for both ISRU and habitat systems as shown in Figure 8a. The optimal PV array area is observed to be in the order of $10^2\ m^2$ as shown in Figure 8f. The mass of the PV array considering the mass of both the array blanket and the array structure is found using the following equation[4]:

$$M_{PV} = (\sigma_a + \sigma_s)\, A_a \tag{4}$$

where A_a is the PV array area, σ_a is the areal density of the multi-junction PV array and σ_s is the estimated array

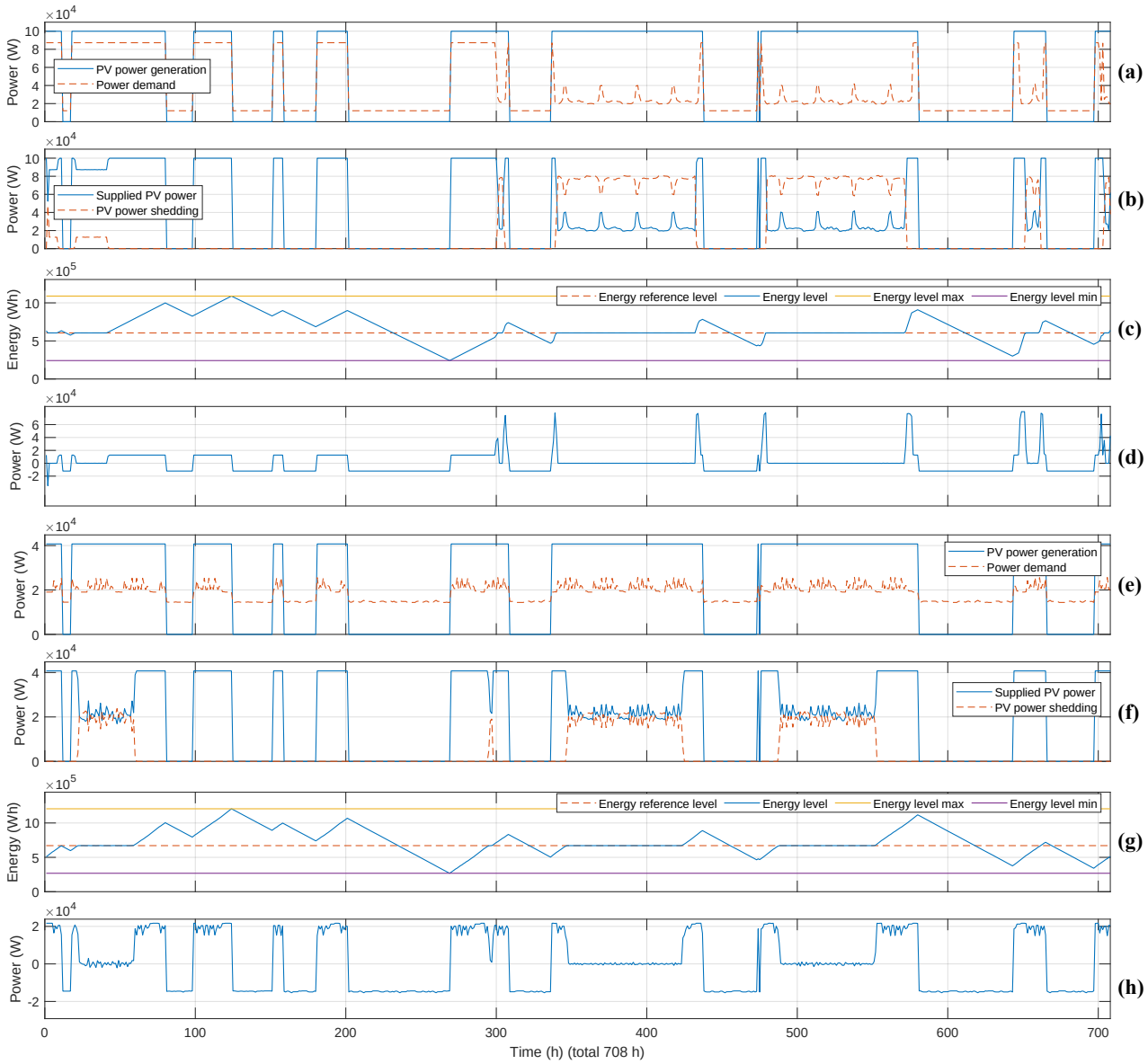

Figure 7. (a) ISRU MG optimal PV array power generation at site #4 with array area of 294.95 m^2 and power demand profile (b) Supplied PV power to ISRU MG and excess PV power curtailment profile to maintain the battery reference at 50% (c) ISRU MG battery SoC profile to maintain the battery reference at 50% (d) ISRU MG battery charging/discharging power profile to maintain battery reference at 50% (e) Habitat MG optimal PV array power generation at site #4 with array area of 120.28 m^2 and power demand profile (f) Supplied PV power to habitat MG and excess PV power curtailment profile to maintain the battery reference at 50% (g) Habitat MG battery SoC profile to maintain the battery reference at 50% (h) Habitat MG battery charging/discharging power profile to maintain battery reference at 50%.

structure specific mass set to 1.59 kg/m^2 and 0.55 kg/m^2, respectively[4]. It is observed that the PV mass is in the order of 10^3 kg for individual ISRU and habitat MGs and also for the integrated system as shown in Figure 8b.

The average illumination and the longest night duration of the 15 candidate sites are shown in Figure 8c and Figure 8d, respectively. It is observed that although the average illumination of sites #3 and #9 is close to 70%, the battery size and mass of these sites are more than site #4. Along with the average illumination, it is observed that the longest night duration plays a vital role in deciding the battery size and mass of the MG. The longest night duration of sites

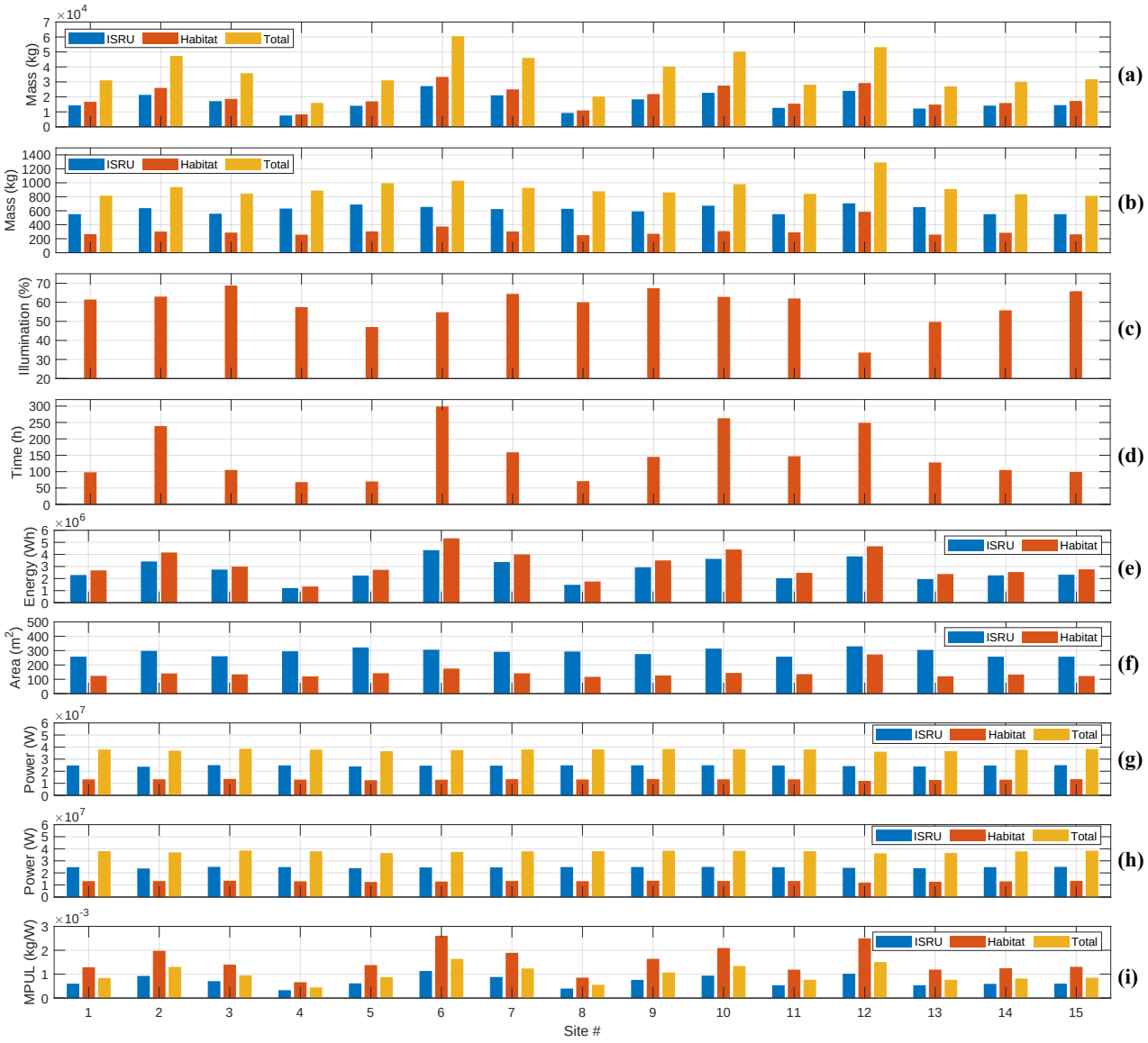

Figure 8. Comparison of 15 sites in terms of (a) battery mass (b) PV array mass (c) average illumination from July 6, 2023, to August 5, 2023 (d) longest night duration from July 6, 2023, to August 5, 2023 (e) battery energy (f) PV array area (g) total power demand served (h) total PV power supplied (i) mass-per-unit-load (MPUL).

#3 and #9 are 105 h and 145 h, respectively, while it is 68 h for site #4. On the other hand, although site #5 has the longest night duration of 70 h similar to site #4, its average illumination is 47.03%, which is significantly lower than site #4, which is 57.48%. Therefore, the battery size and mass for site #5 are higher compared to site #4 even though both sites have a similar longest night duration. Therefore, both the average illumination and the longest night duration affect the battery size and mass of the MG at each location.

It is observed that the battery mass dominates the mass required to be transported compared to PV array mass for establishing a PV-battery MG on the Moon. Therefore, comparing 15 candidate sites, it is observed from Figure 8a that site #4 has the least battery mass of 7563.46 kg and 8379.9 kg for the ISRU and habitat MGs, respectively, and for the combined ISRU and habitat MGs the total battery mass is 15943.4 kg. Other than site #4, site #8 is the next closest candidate site with a similar battery mass of 9237.65 kg and 10981 kg for the ISRU and habitat MGs, respectively, and for the combined ISRU and habitat MG the total battery mass is 20218.7 kg.

The sites are also compared in terms of total PV array and battery system mass and the total power demand served.

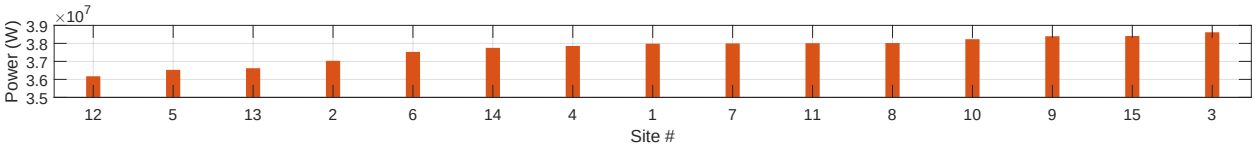

Figure 9. Sites in ascending order of total power demand served.

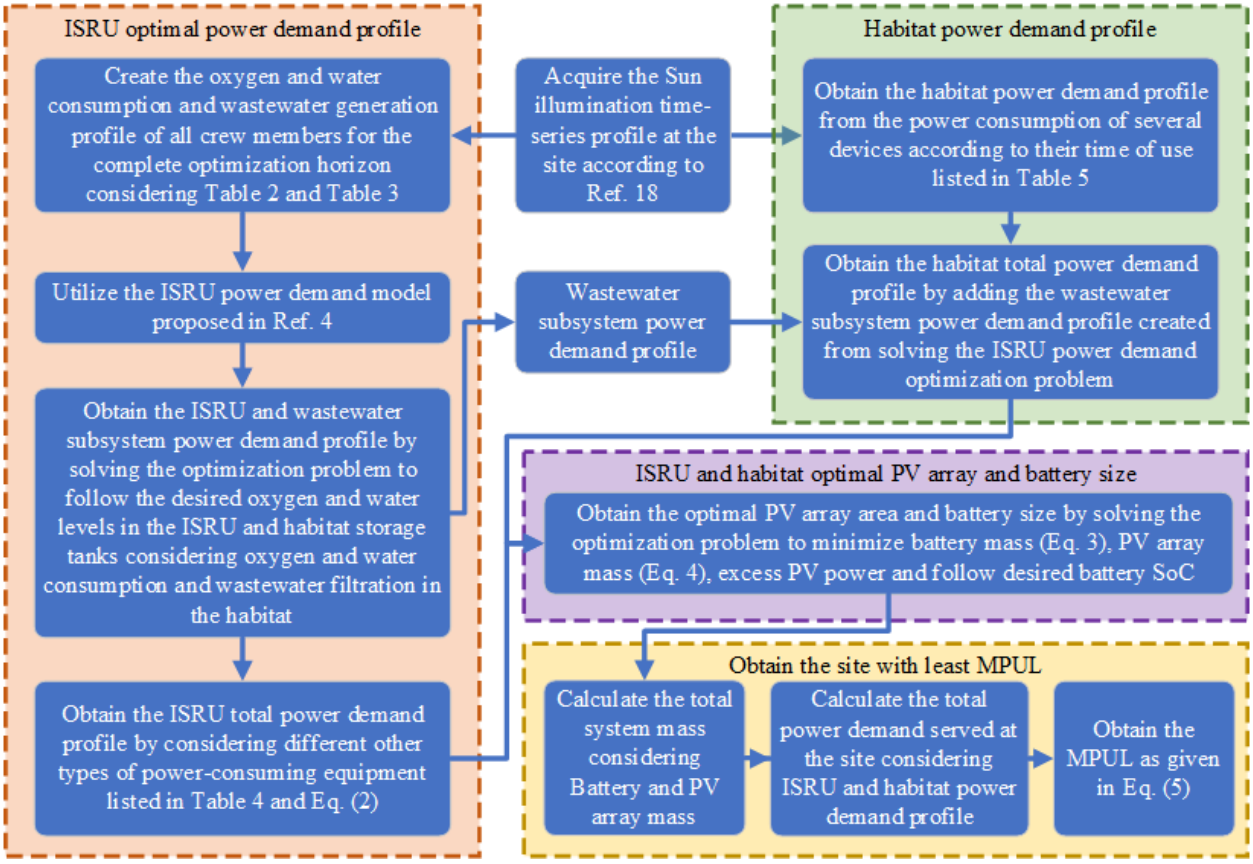

Figure 10. An overview of the workflow to find the site with the least MPUL.

The total power demand served, and the total PV power supplied at the 15 candidate sites are shown in Figure 8g and Figure 8h, respectively. The 15 sites are also sorted in ascending order of total power demand served in Figure 9. It is observed that site #12 and site#3 serve the least and highest total power demand of $36172.84\,kW$ and $38616.949\,kW$, respectively. Therefore, although the 15 candidate sites differ significantly in terms of illumination time-series profile, average illumination conditions and longest night duration, the total power demand served at each site is almost similar.

A criterion based on the ratio of the total mass of the PV-battery system mass to the total power demand served at each site is calculated as given in Eq. (5), called mass-per-unit-load (MPUL), identifies the site serving more power demand with less total system mass.

$$\text{MPUL} = \frac{\text{Total system mass}}{P_L^{total}} \tag{5}$$

where P_L^{total} is the total power demand served during the optimization horizon. The MPUL of the combined ISRU and habitat MGs is calculated using the ISRU and habitat MG's total PV and battery system mass and the ISRU and habitat MG's total power demand served for each site. It is observed that the MPUL for all the sites is in the order of $10^{-3}\ kg/W$ as shown in Figure 8i. The MPUL is the lowest for site #4 at $0.330 \times 10^{-3}\ kg/W$ and $0.662 \times 10^{-3}\ kg/W$ for the ISRU and habitat MG, respectively and for the integrated ISRU and habitat MG the MPUL is $0.444 \times 10^{-3}\ kg/W$. The workflow to determine the optimal ISRU power demand profile, habitat power demand

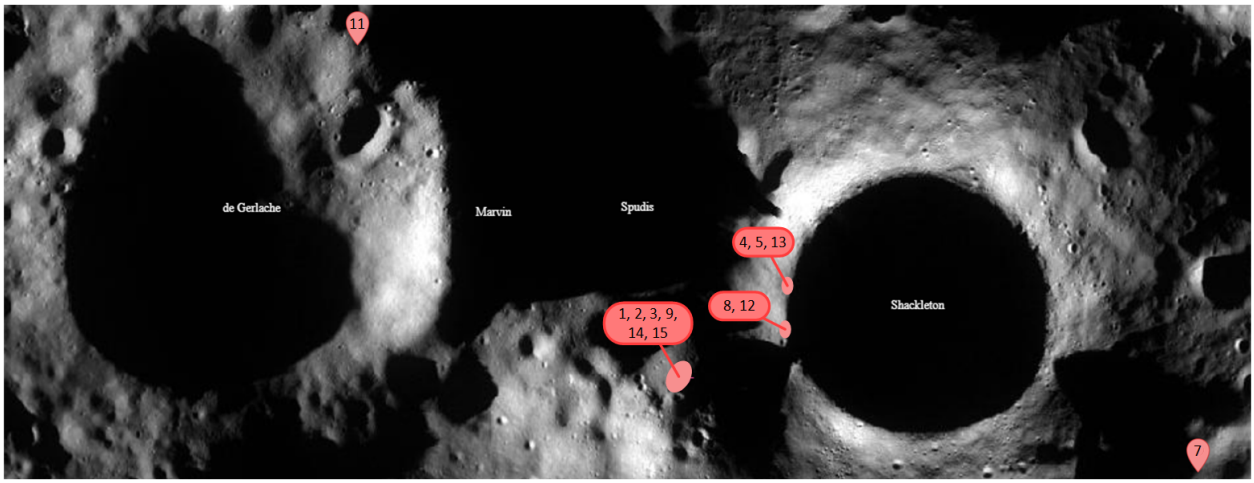

Figure 11. Approximate location of 15 candidate sites listed in Table 1 near the lunar south pole Shackleton crater.[26]

profile, optimal PV and battery size, and the MPUL is shown in Figure 10.

From this analysis, it is concluded that the PV and battery size and mass of a PV-battery based MG depend on both the average illumination and the longest night duration as battery energy is required to supply the power demand during dark periods. However, the average illumination and longest night duration do not significantly affect the total power demand served at each site. It is observed that the battery mass significantly dominates the total PV-battery system mass. It is also observed that the habitat MG requires more battery than the ISRU as there are more critical loads in the habitat than the ISRU. The ISRU power management system prepares the MG for the dark periods by storing more oxygen and water in the respective ISRU tanks to reduce the power consumption from the batteries during dark periods. The PV array area and mass for ISRU MG is more than the habitat MG as it is one of the highest power-consuming units during the daytime to generate the required oxygen and water for the crew members. The approximate location of each site listed in Table 1 is shown in Figure 11. According to previous studies, the rim of the Shackleton crater is highly illuminated, which makes it suitable for establishing a lunar base. In this paper, it is observed that sites #4 and #8, located on the rim of the Shackleton crater, have the lowest battery mass and the minimum MPUL.

V. Conclusion

In this paper, a comparison study was performed to investigate the optimal mass and size of the PV and battery systems, average illumination, longest night duration, total power demand served, and total PV power supply at 15 highly-illuminated sites near the lunar south pole considering a horizon of one month. In the comparison study, separate MGs were considered for ISRU and crew habitat, each having its own PV and battery systems. The power generation profile of the PV system was determined using the Sun illumination time-series profile at these candidate sites and assuming that PV arrays are installed on $10\ m$ high towers. In addition, to model the power demand profile of the ISRU MG, the oxygen and water consumption of the crew members were considered taking into account their daily activities. The power demand profile of the habitat MG was determined considering the power consumption profile of the wastewater filtration subsystem and the power consumed by several equipment in the habitat. It was observed that the optimal size of the PV array and battery size and mass depend on both the average illumination and the longest night duration at each site. Among the 15 studied sites, the winning site showed the least battery mass of $7563.46\ kg$ and $8379.9\ kg$ for the ISRU and habitat MGs, respectively. The PV array mass, considering the mass of the array blanket and the array structure at this site, is $631.61\ kg$ and $257.40\ kg$ for the ISRU and habitat MGs, respectively. Finally, the sites were compared based on the ratio of total PV-battery system mass to the total power demand served, called mass-per-unit-load (MPUL), to identify the sites serving more power demand with less total system mass. It was observed that the winning site has the least MPUL of $0.330 \times 10^{-3}\ kg/W$ and $0.662 \times 10^{-3}\ kg/W$ for the ISRU and habitat MGs, respectively.

References

[1] Saha, D., Bazmohammadi, N., Raya-Armenta, J. M., Bintoudi, A. D., Lashab, A., Vasquez, J. C., and Guerrero, J. M., "Space Microgrids for Future Manned Lunar Bases: A Review," *IEEE Open Access Journal of Power and Energy*, Vol. 8, 2021, pp. 570–583. doi:10.1109/OAJPE.2021.3116674.

[2] Saha, D., Bazmohammadi, N., Raya-Armenta, J. M., Bintoudi, A. D., Lashab, A., Vasquez, J. C., and Guerrero, J. M., "Optimal Sizing and Siting of PV and Battery based Space Microgrids near the Moon's Shackleton Crater," *IEEE Access*, 2023. doi:10.1109/ACCESS.2023.3239303.

[3] Bintoudi, A. D., Timplalexis, C., Mendes, G., Guerrero, J. M., and Demoulias, C., "Design of Space Microgrid for Manned Lunar Base: Spinning-in Terrestrial Technologies," *2019 European Space Power Conference, ESPC 2019*, IEEE, 2019. doi:10.1109/ESPC.2019.8932024.

[4] Colozza, A. J., "Small Lunar Base Camp and In Situ Resource Utilization Oxygen Production Facility Power System Comparison," 2020. URL `https://ntrs.nasa.gov/citations/20200001622`.

[5] Choi, S. H., King, G. C., Kim, H.-J., and Park, Y., "Electrostatic Power Generation from Negatively Charged, Simulated Lunar Regolith," 2010. URL `https://ntrs.nasa.gov/citations/20100032922`.

[6] Kerslake, T. W., "Lunar Surface-to-Surface Power Transfer," *AIP Conference Proceedings*, Vol. 969, American Institute of Physics, 2008, pp. 466–473.

[7] Mazarico, E., Neumann, G., Smith, D., Zuber, M., and Torrence, M., "Illumination conditions of the lunar polar regions using LOLA topography," *Icarus*, Vol. 211, No. 2, 2011, pp. 1066–1081.

[8] Gläser, P., Oberst, J., Neumann, G., Mazarico, E., Speyerer, E., and Robinson, M., "Illumination conditions at the lunar poles: Implications for future exploration," *Planetary and Space Science*, Vol. 162, 2018, pp. 170–178.

[9] Speyerer, E. J., and Robinson, M. S., "Persistently illuminated regions at the lunar poles: Ideal sites for future exploration," *Icarus*, Vol. 222, No. 1, 2013, pp. 122–136.

[10] Fincannon, J., "Characterization of lunar polar illumination from a power system perspective," *46th AIAA Aerospace Sciences Meeting and Exhibit*, 2008, p. 447.

[11] Pappa, R., Taylor, C., Warren, J., Chamberlain, M., Cook, S., Belbin, S., Lepsch, R., Tiffin, D., Doggett, B., Mikulas, M., Wong, I., Long, D., Steinkoening, D., Pensado, A., Blandino, J., and Haste, J., "Relocatable 10 kW Solar Array for Lunar South Pole Missions - NASA Technical Reports Server (NTRS)," , Mar 2021. URL `https://ntrs.nasa.gov/citations/20210011743`, (Accessed on 12/12/2022).

[12] Mueller, R. P., "Lunar Base Construction Overview - NASA Technical Reports Server (NTRS)," , Jan 2022. URL `https://ntrs.nasa.gov/citations/20220000418`, (Accessed on 12/12/2022).

[13] Freeh, J., "Analysis of Stationary, Photovoltaic-Based Surface Power System Designs at the Lunar South Pole," *AIAA SPACE 2008 Conference & Exposition*, 2009, p. 7810.

[14] Fincannon, H. J., "Lunar Environment and Lunar Power Needs," 2020, pp. 1–5. URL `https://ntrs.nasa.gov/citations/20205002224`.

[15] Smith, D. E., Zuber, M. T., Neumann, G. A., Lemoine, F. G., Mazarico, E., Torrence, M. H., McGarry, J. F., Rowlands, D. D., Head III, J. W., Duxbury, T. H., Aharonson, O., Lucey, P. G., Robinson, M. S., Barnouin, O. S., Cavanaugh, J. F., Sun, X., Liiva, P., Mao, D.-d., Smith, J. C., and Bartels, A. E., "Initial observations from the Lunar Orbiter Laser Altimeter (LOLA)," *Geophysical Research Letters*, Vol. 37, No. 18, 2010. doi: https://doi.org/10.1029/2010GL043751.

[16] Barker, M. K., Mazarico, E., Neumann, G. A., Smith, D. E., Zuber, M. T., and Head, J. W., "Improved LOLA elevation maps for south pole landing sites: Error estimates and their impact on illumination conditions," *Planetary and Space Science*, 2020, p. 105119. doi:https://doi.org/10.1016/j.pss.2020.105119.

[17] Fincannon, J., "Lunar South Pole illumination: review, reassessment, and power system implications," *5th International Energy Conversion Engineering Conference and Exhibit (IECEC)*, 2007, p. 4700.

[18] Armenta, J. M. R., Bazmohammadi, N., Saha, D., Vasquez, J. C., and Guerrero, J. M., "Optimal Multi-Site Selection for a PV-based Lunar Settlement Based on A Novel Method to Estimate Sun Illumination Profiles," *Advances in Space Research*, 2023. doi:https://doi.org/10.1016/j.asr.2022.12.048.

[19] Ewert, M. K., Chen, T. T., and Powell, C. D., "Life support baseline values and assumptions document - NASA Technical Reports Server (NTRS)," , Feb 2022. URL `https://ntrs.nasa.gov/citations/20210024855`.

[20] Kaczmarzyk, M., Starakiewicz, A., and Waśniowski, A., "Internal heat gains in a lunar base—a contemporary case study," *Energies*, Vol. 13, No. 12, 2020, p. 3213.

[21] Barta, D. J., Pickering, K. D., Meyer, C., Pensinger, S., Vega, L., Flynn, M., Jackson, A., and Wheeler, R., "A biologically-based alternative water processor for long duration space missions - NASA Technical Reports Server (NTRS)," , May 2015. URL `https://ntrs.nasa.gov/citations/20150014482`.

[22] Meyer, C. E., Pensinger, S., Adam, N., Pickering, K. D., Barta, D., Shull, S. A., Vega, L. M., Lange, K., Christenson, D., and Jackson, W. A., "Results of the alternative water processor test, a novel technology for exploration wastewater remediation," *International Conference on Environmental Systems*, 2016.

[23] Barta, D. J., Wheeler, R., Jackson, W., Pickering, K., Meyer, C., Pensinger, S., Vega, L., and Flynn, M., "An Alternative Water Processor for Long Duration Space Missions," *40th COSPAR Scientific Assembly*, Vol. 40, 2014, pp. F4–2.

[24] Volpin, F., Badeti, U., Wang, C., Jiang, J., Vogel, J., Freguia, S., Fam, D., Cho, J., Phuntsho, S., and Shon, H. K., "Urine treatment on the international space station: current practice and novel approaches," *Membranes*, Vol. 10, No. 11, 2020, p. 327.

[25] Carter, D. L., "Status of the Regenerative ECLSS Water Recovery System," *SAE Technical Papers*, 2009. doi: 10.4271/2009-01-2352.

[26] Arizona State University (ASU), and NASA, "LROC :: QuickMap," , 2023. URL `https://quickmap.lroc.asu.edu/`, (Accessed on 16/2/2023).